

pubs.acs.org/cm Perspective

# Light-Directed Organization of Polymer Materials from Photoreactive Formulations<sup>†</sup>

Ian D. Hosein\*



Cite This: Chem. Mater. 2020, 32, 2673–2687



**ACCESS** 

Metrics & More

Article Recommendations

ABSTRACT: This perspective presents a recently developed approach to organize polymer and polymer composite materials through a new form of light-directed organization of photoreactive polymeric media. Under suitable conditions, such media will interact with light, in a mutual dynamic process, that results in the spontaneous organization of both the input light field and, importantly, the polymer media. New material structures can be created in free-radical-initiated media, polymer blends and polymer—solvent mixtures, as well as possibly more complex, multicomponent formulations. An overview of the underlying principles and chemical phenomena and exemplary material structures are presented. Materials produced using this new processing approach can be used as functional coatings, textured

Normal Light
Divergence
Divergence-Free Waves

Light-Directed Polymer Organization

surfaces, and membranes, as well as a host of other applications via selection of polymer composition. Key open questions and areas for further inquiry and advancement are presented. Coupling the dynamics of light pattern formation processes to photoreactive matter is a promising new approach to the organization of materials for a range of critical applications and reveals interesting nonlinear dynamic phenomena in the organization of materials.

#### 1. INTRODUCTION

A core principle in the advancement of materials science and materials chemistry is the discovery of new processing-structure—property relationships. Every synthesized or processed material system has underlying reactive, diffusive, and dynamic phenomena spanning from the atomic to the macro scale by which the resultant material obtains its structure. Through an understanding of such processes, as they relate to controllable, determinative factors (e.g., concentration, application of stimuli such as heat, electric, catalysts, mechanical agitation, other forms of energy, and time) researchers can finely tune the processes toward the reliable production of materials with the desired structure, which in turn allows for their properties to be explored and engineered for applications.

Over the past century, in what could be term termed the "Polymers Age", polymer materials have reached unmatched ubiquity in terms of their penetration in products, industries, and applications. One of the core reasons is the expansive degrees of freedom available in polymer composition through which structure—property relations may be explored. Examples of such degrees of freedom include monomer composition and structure (backbone as well as side functionalities), molecular weight, and macromolecular architecture (i.e., linear, dendrimer, cross-linked), as well as innumerable combinations and

In terms of the three key elements (reaction, diffusion, and dynamics), polymers may be synthesized using a range of approaches, include free-radical, cationic, anion, reversible addition—fragmentation chain-transfer (RAFT), and atom transfer radical polymerization (ATRP). Such reactive systems can be initiated either under spontaneous ambient conditions or with the application of heat, electromagnetic radiation, electric field, pH, etc. The discovery of new processing approaches, particularly ways to stimulate diffusion and dynamic phenomena, is of fundamental interest for revealing new ways to organize polymer materials. Such approaches would in principle stimulate or amplify concentration gradients as well as drive the diffusion

Received: December 27, 2019 Revised: March 4, 2020 Published: March 4, 2020



<sup>&</sup>lt;sup>†</sup>This Perspective is part of the *Up-and-Coming* series.



arrangements of different mixed polymer components either as composites or chemically linked (i.e., copolymers). In addition to their structural diversity, polymers exhibit a wide range of physical, chemical, and biological properties and thus have found applications spanning from energy conversion and storage to biomedical applications.

and dynamics of the constituent components (i.e., monomers, oligomers, inert materials) in such a way that may be controlled by processing parameters.

One general approach that has shown immense success is to couple polymer materials to other well-known nonlinear dynamic systems. <sup>2,3</sup> Some examples are shown in Figure 1.

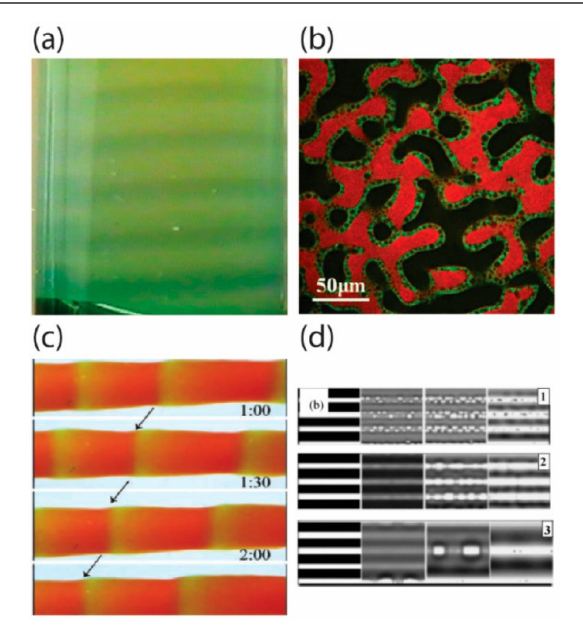


**Figure 1.** Examples of nonlinear dynamics in polymer systems that leads to different pattern and structural formation processes. (a) Thermal polymerization in a free-radical systems. Adapted with permission from ref 4. Copyright 1998 Royal Society of Chemistry. (b) Phase separation in a polymer blend stimulated by irradiation. Adapted with permission from ref 5. Copyright 2014 American Chemical Society. (c) Oscillatory gels coupled to BZ reactions. Adapted with permission from ref 6. Copyright 2008 Wiley. (d) Dewetting of polymer solutions from pattern substrates. Adapted with permission from ref 7. Copyright 2011 Elsevier.

(A) Frontal polymerization is characterized by a moving thermal front driven by the exothermic nature of free-radical polymerization of monomers with high enthalpies. (B) The well-known spinodal decomposition observed for decades in bimetallic alloys is also observed in polymer blends, driven by the chemical dissimilarity of the components to segregate into individually composed phases that create a broad diversity of morphologies. (C) Oscillatory gels result from Belousov—Zhabotinsky reactions, owing to the periodic nature of forming concentration profiles. (D) The dewetting of a solvent from a surface, now with a polymer solution, shows similar hierarchical structures owing to differences in the slip of the contact line along the liquid—solid interface.

A recent observation was of coupling of polymeric materials to the nonlinear dynamics observed in transmitted optical fields.  $^{8,9}$  Initially observed in inorganic media, materials can display strong polarizability on exposure to high-intensity electromagnetic radiation. Known as the Kerr effect, the optical nonlinearity entails a change (particularly an increase) in the refractive index (n) in response to an applied electric field, which may be expressed in the form of a Taylor series expansion in powers of the electric field  $^{10}$ 

$$n(E) = n_0 + n_2 \overline{E}^2 + \dots {1}$$

where  $n_0$  is the linear refractive index,  $n_2$  is the optical Kerr coefficient, and E is the instantaneous electric field of transmitted light. The over bar for E denotes that the nonlinear portion of the refractive index response is related to the time-averaging electric field. Typical materials that display Kerr nonlinearity are found in semiconductors (e.g., aluminum gallium arsenide, AlGaAs), polymers (e.g., p-toluenesulfonate), and glasses (e.g., SiO<sub>2</sub>), as well as in gases and liquids. The Kerr effect is observed at very high light intensities ( $\sim 1 \text{ W/cm}^2$  and up  $1 \text{ GW/cm}^2$ ). As a result of this optical nonlinearity, a variety of optical waveforms and pattern formation processes occur. Their formation entails a dynamic process described by the nonlinear paraxial wave equation for transmitted light  $^{11,12}$ 

$$ik_0 n_0 \frac{\partial \varepsilon}{\partial z} + \frac{1}{2} \nabla_t^2 \varepsilon + k_0^2 n_0 \Delta n \varepsilon + \frac{i}{2} k_0 n_0 \alpha \varepsilon = 0$$
 (2)

where  $\varepsilon$  is the electric field amplitude,  $\alpha$  is the attenuation coefficient of the medium,  $n_0$  is the initial refractive index, and  $k_0$  is the free space wave vector. Inherent in this expression for nonlinear wave propagation is a competition between (1) the natural tendency of a light beam to diverge in the directions orthogonal to its propagation path (transverse Laplacian:  $\nabla_t^2 = \frac{\partial^2}{\partial x^2} + \frac{\partial^2}{\partial y^2}$ ) and (2) a self-focusing nonlinearity due to light-stimulated refractive index changes,  $\Delta n$ , along the propagation path length. One interesting phenomenon that emerges are self-trapped beams, essentially nonlinear waveforms propagating divergence free in their own self-stimulated optical waveguide. Self-trapped beams emerge through a dynamic balance between the natural divergence of light and this new self-focusing nonlinearity (Figure 2).

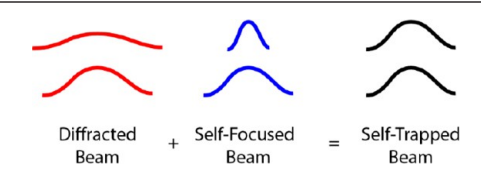


**Figure 2.** Schematic of self-trapping of light illustrated by the radial cross section of a Gaussian beam (propagating upward). Light naturally diverges along its propagation path (red). In a nonlinear optical medium, self-focusing causes the optical beam to narrow, or focus, onto itself (blue). A dynamic balance between divergence and self-focusing leads to self-trapping (black). Reprinted with permission from ref 13. Copyright 2017 American Institute of Physics.

Optical nonlinearity enters into the realm of polymer materials, particularly photoinitiated media, owing to the (photo)polymerization leading to increases in refractive index. Namely, the refractive index of polymers increases with the associated densification of the media owing to the increase in molecular weight from the growing polymer backbone, as well as any possible conformational changes associated with the aggregation of growing chains, either through van der Waals forces or through chemical cross-linking. The bridge to optical nonlinearity is the well-known intensity dependence of photopolymerization, 15,16 and thus the refractive index change in photopolymer media is also intensity dependent and can be generally expressed by

$$n(x, y, x, t) = n_{\rm m} + \Delta n(x, y, z, t)$$
 (3)

The change in refractive index  $\Delta n$  can be expressed as

$$\Delta n(x, y, z, t) = \Delta n_{s} \left\{ 1 - \exp \left[ -\frac{1}{U_{o}} \int_{0}^{t-\tau} |E(t')|^{2} dt' \right] \right\}$$
(4)

where  $\Delta n_s$  is the maximum attainable index change (between maximally cured and uncured photopolymer media),  $U_0$  is the critical energy density to initiate polymerization (units of J/cm²),  $\tau$  is the monomer radical lifetime, and E(t) is the electric field amplitude of the irradiating field. Equation 2 describes the strength of the nonlinearity,  $\Delta n_s$ , as being specifically dependent on the light intensity, the efficiency/rate of the photopolymerization reaction, and the term  $\Delta n_s$  is associated with the final, most dense structure attained by the polymer media, entailing dependences spanning from molecular to macromolecular conformations.

One key phenomenon in such nonlinear dynamics, particularly now in photoreactive systems, is the positive feedback between light intensity and photopolymerization rate. Namely, light stimulates a polymerization-induced rise in refractive index. Then optical energy from surrounding regions refract into this region, thereby raising the local irradiation dosage, which further increases photoinitiation and polymerization, thereby completing the positive feedback loop. This leads to what has been termed optical autocatalysis, <sup>17</sup> similar to thermal autocatalysis, <sup>18</sup> where in the former the increase in polymer refractive index establishes the feedback loop, and in the latter the heat produced in the reaction establishes the loop. Particularly, the optical autocatalytic effect leads to a mutual dynamic interaction between light and the underlying polymer media, whereby light begins to "self"-focus, and polymer growth is concentrated to this focused region. As a result, it also stimulates spatially dependent diffusion and dynamic processes in the polymer media, owing to the localization of polymerization in the selffocused region. This photopolymerization-induced nonlinearity is obtained with optical powers generally between 1 and 100 mW/cm<sup>2</sup>, well below that needed to elicit the phenomenon in inorganic media. As well, the slow chemical reaction (i.e., noninstantaneous response) associated with polymers allows incoherent sources (i.e., incandescent sources, LEDs, even sunlight) to elicit nonlinearity, because any inherent spatial or temporal noise in the source is canceled out from the timeaveraged intensity profile that actually affects the polymer reaction. Another benefit of this phenomenon, from a processing standpoint, comes from using radiation curing to elicit it, owing to irradiation of photoreactive media being of low energy, low cost, and nondestructive, as well as applicable to both open and closed systems (i.e., through a transparent window). 19,20 Radiation curing is widely employed to synthesize materials for applications in thin films, coatings, printing, dentistry, optics, and electronics.

### INITIAL WORK ON THE COUPLING OF NONLINEAR OPTICAL DYNAMICS TO POLYMER SYSTEMS

The self-focusing phenomenon was observed previously, as shown in Figure 3, for both UV as well as a visible (blue) laser light. Figure 3a specifically shows the self-focusing of light over time, revealing how the focal point moves toward the entry location of light due to the increasingly stronger light focusing from the associated higher refractive index. Figure 5b shows an example of an initially spatially divergent beam undergoing a dynamic balance with self-focusing, resulting in divergence-free propagation of the optical beam over across the medium.

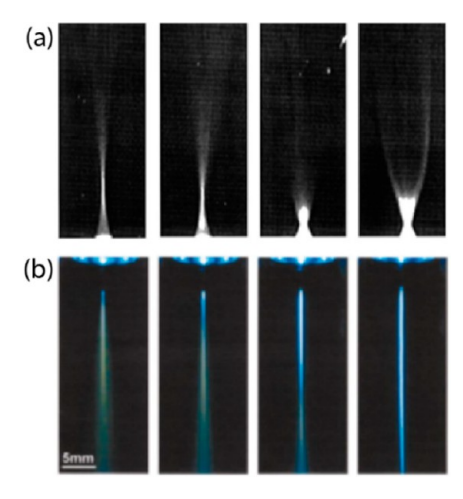


**Figure 3.** Self-focusing of a microscale optical beam in photopolymers over the course of irradiation. Successive images in each row show the change in the beam profile over its propagation path over the course of irradiation. (a) Self-focusing of a UV laser beam ( $\lambda=325$  nm) in a photo-cross-linking acrylate. Reprinted with permission from ref 8. Copyright 1996 Optical Society of America. (b) Self-trapping of a visible light laser ( $\lambda=488$  nm) in a photopolymerizing mixture. Reprinted with permission from ref 21. Copyright 2001 American Institute of Physics.

Similarly, self-trapping (or filamentation) of incandescent beams has also been observed (Figure 4).<sup>22</sup> Such systems were photosensitized to blue light, yet it was shown that all wavelengths of the polychromatic spectrum undergo self-trapping and response to the increase in refractive index.

Owing to the permanence of the photopolymerization, from a materials point of view, the sustained irradiation results in the growth of an individual polymer structure in the shape of a fiber whose length increases owing to the propagation of the tip into the resin (Figure 5a), with subsequent light traveling along the formed fiber to the very tip, thereby sustaining growth. Hence, self-focusing occurs continuously and dynamically at the tip as it grows into the medium, and the fiber is built by the assembly of polymerizing chains at its end. The fiber may continue to grow to the end of the medium or may slow down and even cease owing to the consumption of optical energy across the fiber length, as well as limited monomer diffusions to the tip, relative to the increasing area of its periphery (side walls), which results in the fibers growing slightly in diameter. Hence, this nonlinear optical process becomes a tool for inscribing permanent microstructure in a photoreactive polymer medium, particularly through the inscription of microscale "rods" or "fibers". <sup>23,24</sup> For example, irradiating a resin with a laser beam and rastering its position along the transverse area of a medium can result in the production of arrays of such fibers (Figure 5b), in a processing termed light-induced self-writing.

An important aspect of eliciting nonlinear optical phenomena in photoreactive polymer systems is the capability to use incoherent (both spatially and temporally) light sources, such as incandescent lamps (white light) and light-emitting diodes (LEDs). In traditional nonlinear media, the nonlinear optical response is instantaneous, and hence, the inherent "speckled" nature of incoherent light which fluctuates at the femtosecond scale will cause propagating optical beams to rapidly change their profiles and consequently deteriorate over their propagation path. However, the optical response of photoreactive systems is *noninstantaneous*, owing to the slow rate of the

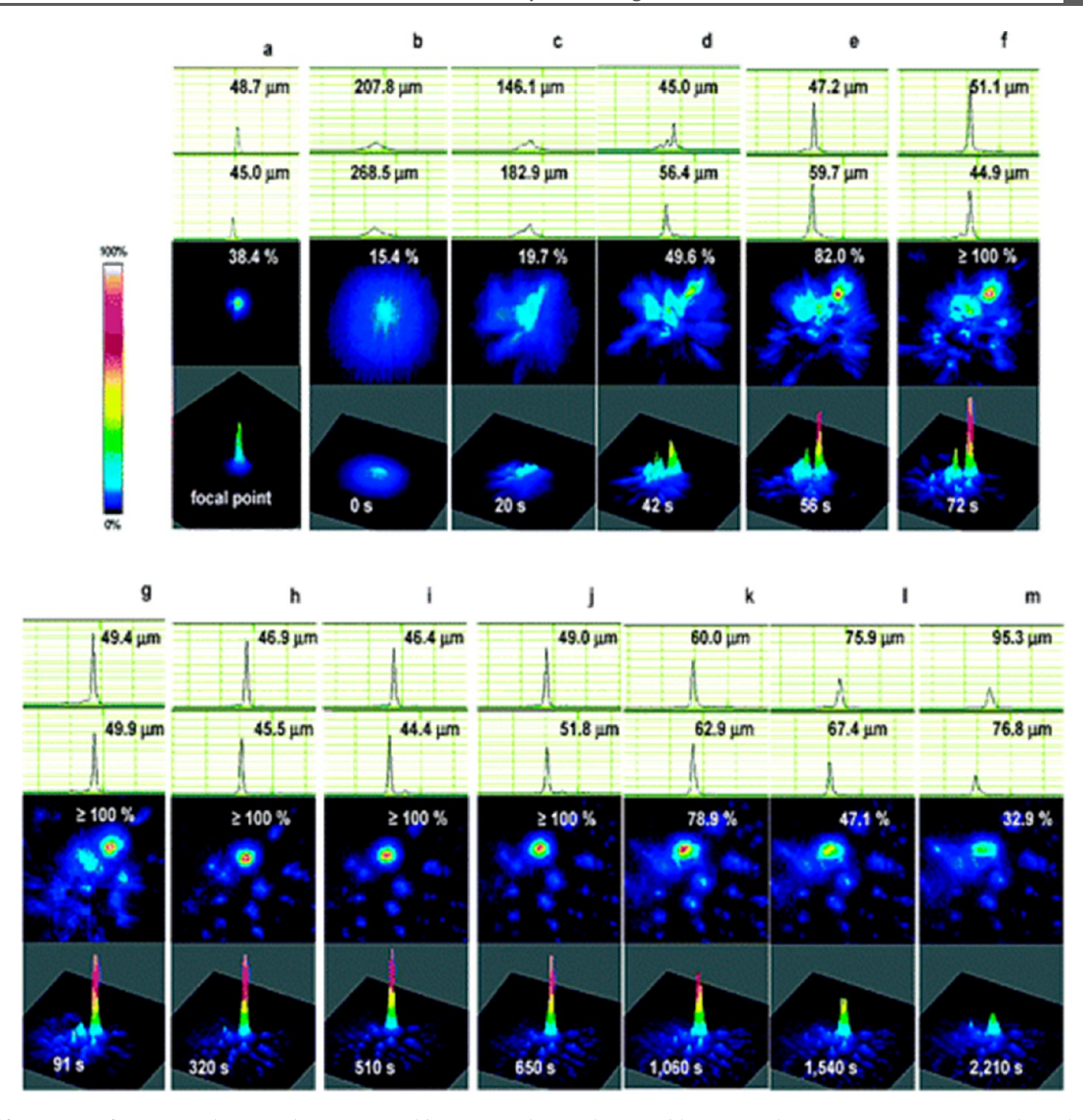


Figure 4. Self-trapping of a microscale, incandescent optical beam in a photopolymerizable organosiloxane. Successive images show the evolution of the spatial profile of the transmitted beam. Reprinted with permission from ref 22. Copyright 2006 American Chemical Society.

photoinduced reaction (over the millisecond scale), which in turn has a slow response to the optical field. As a result, the medium responds to the time-averaged intensity profile of light, over which the rapid fluctuations in the incoherent light sources are not experienced by the medium. Hence, incoherent optical beams can undergo self-trapping, and their preserved self-trapped profiles can proceed to direct the patterning and organization of polymer materials. Additionally, the refractive index changes  $(\Delta n)$  in photopolymer systems are greater  $(\sim 0.01)$  than those for convention nonlinear media  $(\sim 10^{-6})$ , which enables it to support the filamentation of multimodal, multiwavelength light.

# 3. RECENT WORK ON SELF-TRAPPING AND SELF-WRITING POLYMER MATERIALS

Over the course of the past decade, self-trapping in polymers has significantly advanced over the preliminary progress from the late 1990s and mid-2000s. These advances have included the concurrent self-trapping of multiple microscale beams in different photoinitiated media, as well as self-trapping in different polymeric media, such as blends and photopolymer—solvent mixtures. This has led to an understanding of the

underlying photopolymer reaction kinetics, diffusion, and dynamics and the resultant structures, which are discussed herein, as well as a range of functional applications, <sup>24,26–30</sup> whose in-depth discussion is beyond the scope of this perspective.

**3.1. Single-Component Systems.** Beyond the preliminary work on self-trapping in simple diacrylate and acrylate-siloxane molcules, 8,22 self-trapping was observed in a family of photoinitiated acrylate monomer formulations.<sup>31</sup> It was found that cross-linking media was key to allowing the self-trapping process to proceed. Namely, monofunctional or difunctional acrylates would initially elicit self-trapping of arrays of optical beams; however, owing to significant shrinkage of the media (a wellknown observation in lower functional polymeric materials) the locations of the forming polymer structures shifted relative to the input beams, thereby smearing the optical pattern and underlying structure.<sup>31</sup> However, with higher functional monomers with f = 3-5, self-trapping in arrays of optical beams was achieved. An important observation was that lower functional monomers could elicit self-trapping when they are formulated with fractions of higher functional monomers with weight fraction ranges of 5–30%. Figure 6a,b shows examples of

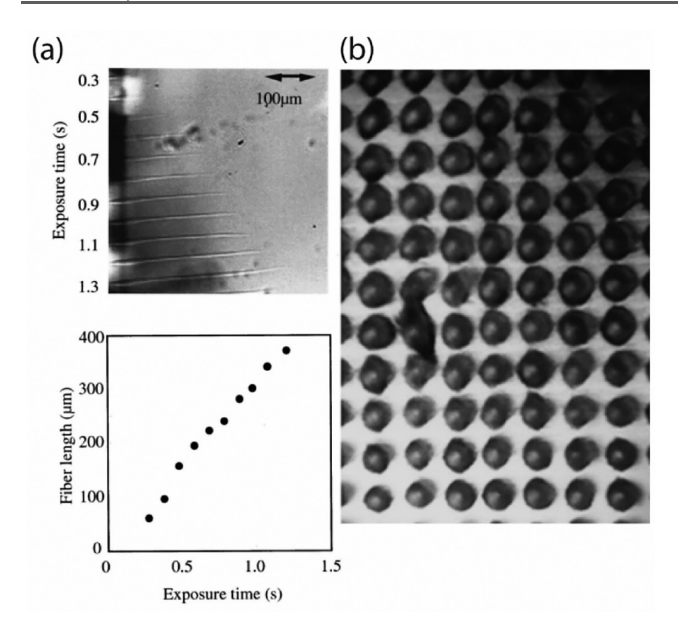


**Figure 5.** Light-induced self-writing of microscale fibers in a photocurable resin. (a) In situ observation of fiber growth over time, and a plot of the fiber length versus exposure time. Reprinted with permission from ref 25. Copyright 1999 American Institute of Physics. (b) Array of self-written fibers formed through exposure of a medium to a microscale laser beam, periodically rastered over the area of the resin, which produces arrays of fibers suspended in the otherwise liquid photopolymer. Adapted with permission from ref 8. Copyright 1996 Optical Society of America.

the pattern formation in both the optical pattern (i.e., self-trapping) and the microstructure (optical microscopy). Polymer pattern formation correlates to the spatial variation in conversion of the formulation, as revealed by 2D Raman

spectroscopic mapping (Figure 6c), which shows intensity regions associated with higher double-bond conversion, which also spatially correlates to the region's self-trapping. Hence, selftrapping is indeed associated with underlying differences in the conversion and, as expected, the diffusion in the monomer content. Similar pattern formations were also observed in cationic systems, photoinitiated using a visible light free-radical initiation that also initiates the cationic initiator through a freeradical-induced decomposition (Figure 6c,d).<sup>32</sup> Both 1D and 2D arrays could be produced. Furthermore, spontaneous formation of randomly positioned self-trapped beams, also referred to as filaments, were also observed in a process referred to as modulation instability (MI),<sup>33</sup> in which inherent spatial noise in the medium seeds the formation of the self-trapped beams. Periodic arrays were pursued thereafter, owing to the regularity of the structure allowing for tunability.

While they are related, divergence-free propagation of individual beams and this phenomenon of modulation instability are distinct phenomena. Self-trapping of an individual optical beam entails a dynamic balance between natural divergence and the self-focusing nonlinearity, leading to divergence-free propagation. However, MI is the spontaneous, stochastic breakup of a wide area optical field into a multitude of filaments. This process is seeded by inherent noise in the optical field, which causes regions of infinitesimally greater intensity to attain an infinitesimally greater refractive index in comparison to its surroundings. This leads to the leakage of light from into this regions, leading to a positive feedback that renders the initially uniform optical field to become unstable, resulting in its breakup. This spontaneous, mask-free formation of self-trapped filaments is attractive over employing a mask (to create 1D or 2D arrays) owing to the scalability of the former. Extremely large scale

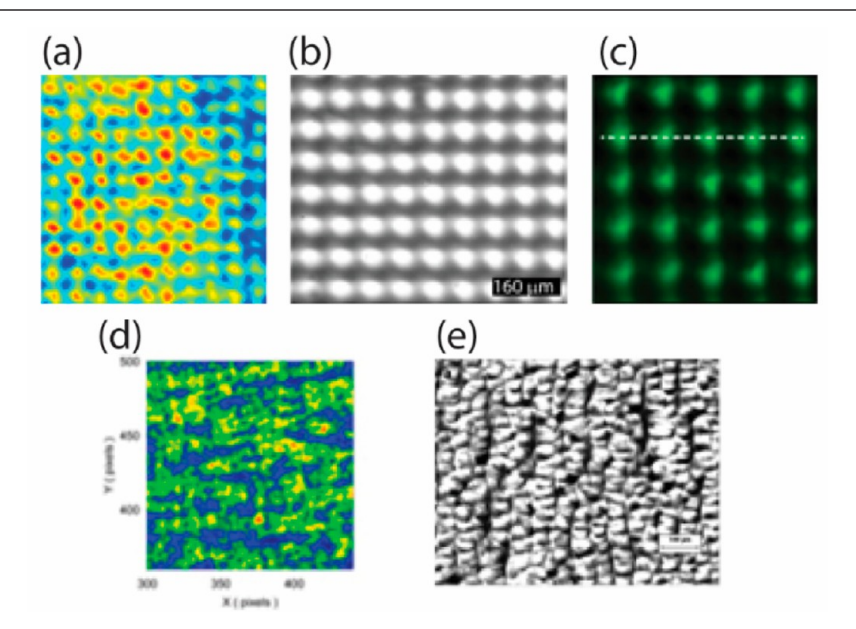


Figure 6. Coupling of light patterning to the underlying photo-cross-linked structure. (a) Spontaneous ordered filamentation of incandescent light in a free-radical-photoinitiated triacrylate media, as revealed from the transverse spatial intensity of transmitted light. (b) Optical microscopy image of the polymer microstructure, wherein bright regions correspond to those with higher degrees of polymerization. (c) Conversion degree evidenced by Raman 2D spectroscopic mapping, revealing correlation of high conversion to the regions of filamentation in the microstructure. Adapted with permission from ref 31. Copyright 2016 American Chemical Society. (d) Spontaneous emergence of self-trapped beams, or filaments, in an epoxide formulation. (e) Corresponding microstructure in the epoxy material. Adapted with permission from ref 32. Copyright 2015 American Chemical Society.

patterning from MI (>10 cm<sup>2</sup>) should be pursued to show the capability of mass-producing these films for applications.

Another interesting observation was that the nonlinear pattern formation occurred within a specific range of irradiation intensities, from 4 to 20 mW/cm<sup>2,31</sup> Lower intensities showed homogeneous curing, and at higher intensities the sample uniformly cross-links as well. Hence, there is an optimal intensity where the changes in the refractive index, induced by irradiation, allow the polymer media to evolve in terms of its molecular weight and morphology to suitably respond to the optical stimulation. At low intensities, the process occurs too slowly relative to dynamic relaxation processes in concentration gradients and molecular weights, so that homogenization of the media is favored over pattern formation. At high intensities, the reaction is so fast the entire medium cross-links, and the expect diffusion of radicals into the dark regions aids in the polymerization of the entire medium, leading to very little differences between the irradiated and nonirradiated regions. This was similar to observations with a single laser beam at very high intensities.8

An open question remains on how the higher functional molecules affect the kinetics of the formation of the structures. It is possible that the greater enthalpies of higher functional molecules and their associated high reactivity could lead not simply to greater  $\Delta n$  values, in the same amount of time, which increases  $d\Delta n_s/dt$  but that the reaction rate is itself faster. It was shown that, with greater  $\Delta n_s$ , the the self-trapping was stronger as quantified by smaller filament sizes, and this was a demonstration of how the nonlinearity could be tuned through polymer formulation.<sup>31</sup> This revealed how underlying polymer formation kinetics and conversion as well as the underlying macromolecular structure can support the increase in refractive index. Detailed kinetic studies on the polymer conversion rate and its correlation to the pattern formation is an open area of study that should be pursued. This should also be performed in conjunction with power-dependent studies, to understand how both photoinitation and formulation changes the rates of growth and how this growth enables pattern formation.

Simulations of the process continue to be extremely insightful to correlating the underlying polymer conversion and dynamic processes. Yariv et al. performed beam propagation simulations in a model photopolymer, updating the refractive index profile with each run based on an integrated total intensity over time. Belgacem and co-workers employed a two-component diffusion model, 37,38 which included the kinetics for the conversion of monomer to polymer (Figure 7). Li and co-workers further accounted for photoabsorptive behavior of the photosensitizing

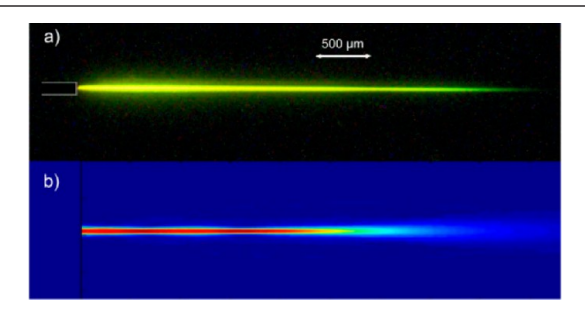


**Figure 7.** (a) Observation of light-induced self-focusing in a photocurable polymer resin. (b) Simulation of the light intensity distribution in the waveguide. Reprinted with permission from ref 39. Copyright 2015 Optical Society of America.

molecule/dye that initiates the reaction during self-writing, thereby accounting for the local spatial concentration variations. Figure 10 shows the correspondence between experimental self-focusing and self-trapping of laser light and complementing simulations of self-trapping.

Thus far, control of the spatial arrangements of the filaments, and thus the symmetry of the resulting structures, has found success by employing different mask patterns, leading for example to 2D and 3D structures possessing various symmetries. 41-44 One question was whether a mask is needed simply to seed the process or for the entire pattern formation process to ensue. Early reports of random filamentation (i.e., modulation instability) show that self-trapped lamellae form first and that this is caused by unseen striations in the glass cells used to contain the formulations. In later studies, a 1D mask consisting of chrome lines was used to force lamellae formation, and spontaneous pattern formation was associated with these lamellae breaking into the individual filaments. Subsequent experiments show that randomly positioned filamentation seeded by the system itself (rather than variations associated with the experimental setup) is possible;<sup>31</sup> however, the individual filaments and their respective optical and micro structures remain to be elucidated in terms of regularity, size, and reproducibility. More recently, experiments observed the phenomenon of spontaneous ordering of filaments produced during MI of two and three nonparallel beams propagated through a medium without the use of any mask (Figure 8).<sup>45</sup>

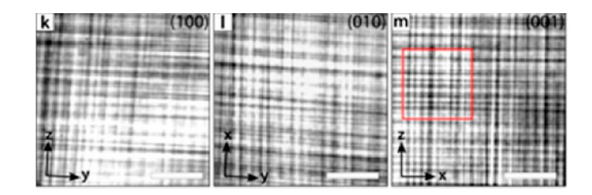


**Figure 8.** Optical microscopy images of 3D lattice (ordered) produced from the simultaneous MI of three orthogonal beams propagated through a photopolymerizable fluid. Images reveal the ordered filaments from the three orthogonal faces zy, xy, and xz, from left to right, respectively. All scale bars are 500  $\mu$ m. Adapted with permission from ref 45. Copyright 2018 American Chemical Society.

This exciting observation demonstrates the potential for a medium to self-direct its organization into regular structures. The capability of producing ordered 2D and 3D arrays of filaments, and in turn 2D and 3D periodic polymer structures, is attributed to the interactions between nearest-neighbor filaments. These findings open opportunities for the large-scale organization of polymer materials, now that the use of a mask may be eliminated. Ordered structures were also produced when multiple light sources were transmitted through a common face of the medium, and this can allow the process to be more practical from a manufacturing standpoint: for example, to enable integrating with roll-to-roll (R2R) processes. Future studies should also focus on further investigating such interactions and the capability of organizing different 2D and 3D arrays with different patterns and symmetries.

In terms of applications, these single or formulated systems have recently found applications as a new class of light-harvesting and light-controlling coatings, owing to their inherent waveguiding properties. The concept is based on the angular acceptance windows of the individual polymer filaments (that operate as the waveguides), which collectively allows the

material to collect light from one incidence angle and redirect its propagation along the filament axes at angles not attainable through simple refraction based on Snell's law. 46,47 This has be exploited toward thin-film coatings for imaging optics, using planar films with intersecting filament array structures (multidirection waveguide lattice) produced by irradiation of a medium with multiple light sources. 48 Media contained in hemispherical containers allow for the production of filaments whose angle of orientation sweeps over a range of angles (i.e., radial waveguide arrays), enabling collection and focusing of light. 49 This has been used to manipulate beam profiles of encapsulated light-emitting diodes (LEDs).<sup>50</sup> Another general application is toward enhanced light collection in solar cells, specifically with the waveguides showing the capability to mitigate shading loss by redirecting light away from front contacts, thereby dramatically increasing conversion efficiency at non-normally incident angles.<sup>51</sup> Thin films have also been produced as a 1D array of slabs, each of which is produced by self-trapping light in predefined positions dictated by a mask.<sup>2</sup> When such arrays of slabs are overlaid on a solar cell, they also redirect light away from front contacts and increase energy conversion. Another approach is through the growth of vertically aligned microfiber optic arrays which can be overlaid on a solar cell, which also increases energy conversion. 52 One other application has used the filaments and their interactions for computing and data storage, with the polymer medium itself able to perform the computations and store information. 53,54

**3.2. Polymer Blends.** Coupling the self-focusing properties of light to polymer blends represents a new approach to directing the morphology of such blends and possibly to directing their morphology to have patterns similar to those of the optical beam arrangements. 13 Specifically, self-trapping can also induce photopolymerization-induced phase separation, in order to direct binary phase morphology. Prior to this work, there were generally two ways to direct the morphology of polymer blends, the first being uniform radiation<sup>55</sup> and the second use of a three-dimensional constructive interference field: namely, holographic lithography. 56 Both approaches provide their respective advantages. In the case of uniform irradiation, the process is scalable, and there are a variety of diverse structures that can be obtained, from spinodal structures to droplet phases, and there is even the possibility of some inherent ordering of the phases. However, the ability to repeatedly attain the same structure remains elusive. In the case of using a three-dimensional holographic field, a high degree of structural order is obtained; however, the scale at which structures can be made is quite limited ( $\sim 1 \text{ cm}^2 \text{ area}$ ,  $\sim 100 \ \mu \text{m}$  depth). Furthermore, the setup is quite complex, requiring up to four separate sources to be used in order to obtain three-dimensional constructive fields. Directing the polymer blend morphology using the self-focusing properties of light seeks to combine the lithographic nature of holography and the scalability of uniform irradiation.

Preliminary studies first examined filamentation (i.e., modulation instability) in photoreactive blends of acrylate and epoxide monomers, each photoinitiated using free-radical polymerization and cationic polymerization, respectively. Filamentation was observed in three different formulations, which varied the functionality of the acrylate monomer from 1 to 3. Filamentation was clearly observed in all structures (Figure 9). The key finding was that the blend phase separates into a binary phase morphology that showed spatial congruence to the optical patterned. Namely, there was a presence of long acrylate-rich

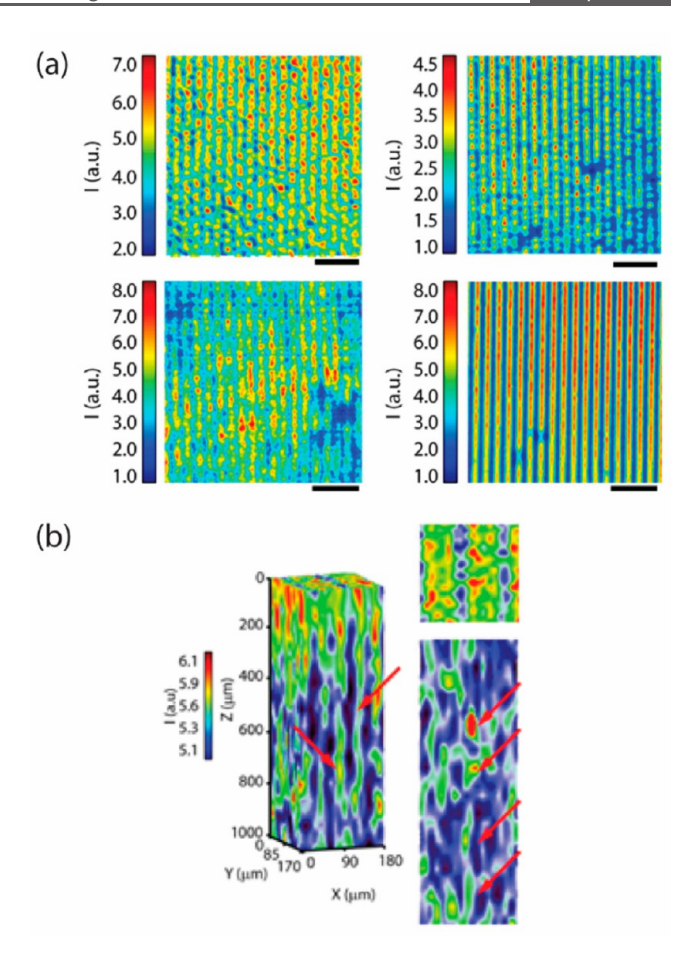


**Figure 9.** Spontaneous filamentation (modulation instability) of incandescent light in photoreactive polymer blends. (a) Resultant pattern for formulations with monoacrylate (top left), diacrylate (top right), and triacrylate (bottom left) monomers as the free-radical component. The bottom right shows the pattern at the beginning of irradiation. (b) Confocal Raman volumes and slices revealing the binary phase morphology. Arrows indicate the presence of an acrylate-rich filament phase. Adapted with permission from ref 17. Copyright 2016 American Chemical Society.

"filament" phases, surrounded by an epoxy matrix occupying the dark regions. This provided the initial evidence that it was possible to have a light pattern direct the binary phase morphology of a polymer blend to have a structure that was spatially congruent to the optical pattern, indicating the possibility for large-scale organization of polymer blends using the nonlinear optical properties of transmitted light. However, such correlated filament phases in the polymer were only observed for diacrylate monomer formulation. Namely, there is an inherent competition between phase separation and crosslinking, the former wanting to separate the two components of the polymer phase and the latter wanting to keep them together. If the drive for phase separation is much stronger than that for cross-linking, then the binary phase morphology might evolve beyond that dictated by the optical filament pattern and no correlated phase morphology is obtained. On the other hand, if cross-linking is strong, a filament-based structure would be present, but there would be an insufficient amount of mobility of the polymer components to allow for phase separation. Hence, this competition is key to determining the final structure, an observation similar to that has shown with blends under uniform irradiation.55

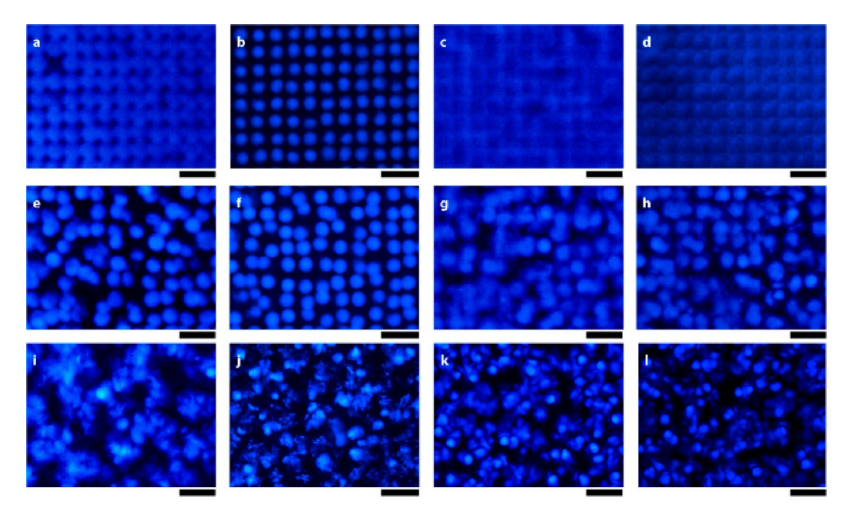


**Figure 10.** Final morphologies observed by an *in situ* study of blends irradiated with an array of self-trapped light beams: (a-d) 90/10; (e-h) 80/20; (i-l) 50/50. Exposure intensities are 1, 5, 10, and 15 mW/cm<sup>2</sup> for columns left to right, respectively. Scale bars: 400  $\mu$ m. Reprinted with permission from ref 62. Copyright 2017 American Chemical Society.

There are several critical properties of the systems whereby such morphologies are achieved: the first being that the faster polymerizing component, namely the acrylate, forms the filaments and the slower reacting component, the epoxy, forms the surrounding matrix. Namely, the faster-growing material will always form the filament, and the more slowly growing material will be expelled into the surroundings. Additionally, the component constituting the filament region must have a higher refractive index, to retain the waveguiding conditions. It remains an open question whether or not these are necessary conditions of the system: that is, whether or not a filament composed of a slower reacting monomer or one with a lower refractive index would allow structures to form. The filamentation process simply needs an increase in refractive index in the medium even if it remains mixed (i.e., not phase separated) and is a combination of the reactions of both the acrylate and epoxy. There was also significant shrinkage in the monoacrylate formulations ( $\sim$ 60%) as well as in the diacrylate and triacrylate formulations (10-15%) with most of the shrinkage occurring in the first 30 min of irradiation, 17 and it is possible that this could disrupt the integrity and spatial locations of the forming filaments. This may be mitigated through performing a uniform irradiative precure of the samples to allow the media to shrink before proceeding with experiments eliciting nonlinear phenomena. Another open question is whether or not when phase separation begins the constituent refractive indices need to be such that there are waveguiding properties.

**3.3. Principles for Formation.** Some further elucidation about the competition of these two processes, phase separation and photo-cross-linking, can be understood in terms of the thermodynamics of the system. The total free energy of a binary blend may be expressed as <sup>57,58</sup>

$$\frac{\Delta G}{RT} = \frac{3}{2N_1} (\varphi_S^{2/3} \varphi^{1/3} - \varphi) + \frac{2\varphi}{fN_1} \ln \left( \frac{\varphi}{\varphi_s} \right) + \frac{(1 - \varphi) \ln(1 - \varphi)}{N_2} + \chi \varphi (1 - \varphi)$$
(5)

where  $\varphi$  is the volume fraction of acrylate,  $\varphi_s$  is the network volume fraction,  $N_1$  and  $N_2$  are the degrees of polymerization for the free-radical component and cationic component, respec-

tively, f is the functionality of TMPTA, and  $\chi$  is the interaction parameter. Equation 5 accounts for polymerization and changes in elasticity and shrinkage of the blend, and shrinkage during irradiation and the associated change in the volume fractions of the blend components can be determined by examining resin heights over time during irradiation, to obtain time-resolved changes in volume fraction. The critical interaction parameter,  $\chi_{\mathcal{O}}$  indicates the point at which spinodal decomposition occurs and is determined when the second derivative of the free energy is equal to zero:

$$\chi_{\rm c} = \frac{1}{2} \left( \frac{2}{f N_{\rm l} \varphi} + \frac{\varphi_{\rm S}^{2/3}}{N_{\rm l} \varphi^{5/3}} + \frac{1}{N_{\rm 2} (1 - \phi)} \right) \tag{6}$$

As  $\chi_{\rm c}$  decreases with increases in  $N_1$  and  $N_2$  over time, the onset of mixing instability is indicated by when  $\chi_{\rm c} < \chi_{\rm FH}$ , where  $\chi_{\rm FH}$  is the Flory–Huggins interaction parameter of the blend determined by the Hildebrand solubility parameters ( $\delta$ ) of the components:

$$\chi_{\rm FH} = \frac{V_{\rm r}}{RT} (\delta_1 - \delta_2)^2 \tag{7}$$

Equation 6 illustrates the inherent competition in the system based on the molecular weights,  $N_1$  and  $N_2$ . As they increase, the decrease in  $\chi_c$  eventually favors phase separation. Photo-crosslinking is not specifically indicated in the equation to some extent by f, but rather by varying the relative weight fraction of the polyfunctional monomer the extent of cross-linking can be varied, and greater fractions will induce greater cross-linking and inhibit the components from separating. Simulations of the process all revealed this competition over a range of parameters. 60 Overall there still remain several studies to be performed on the underlying determinative factors and how they affect the attainment of correlated morphologies. What is known at present is that the faster-reacting component must also be the high refractive index system and ideally what is needed is a crosslinking system to form stable filament phases, which then can expel the lower refractive index component, which is also more slowly reacting, into the matrix. Combinations of other types of high and low refractive index components with and slow and fast polymerization reactions will show whether or not this is true.

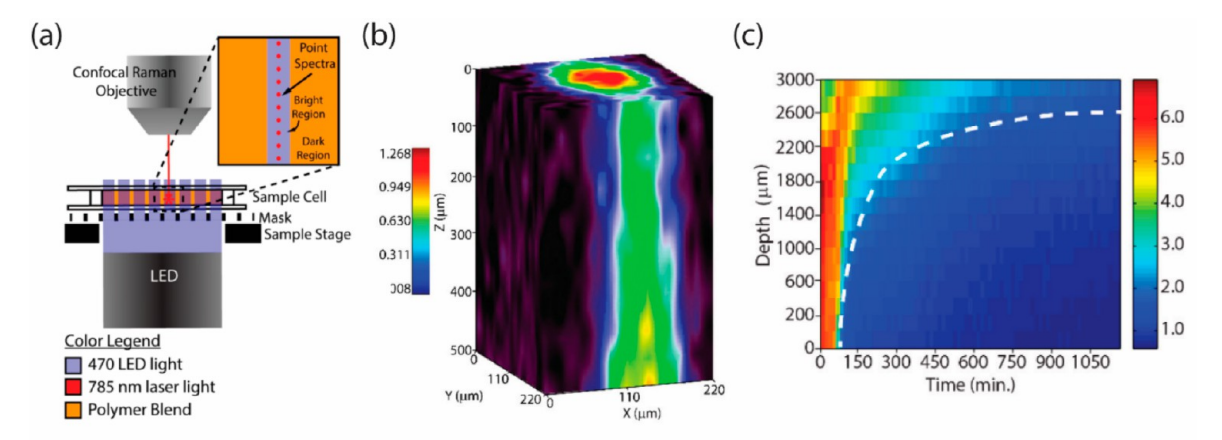


Figure 11. Experimental confocal Raman spectroscopy to track the evolution of polymer blend conversion, morphology, and phase separation during irradiation with visible light beams. (a) Experimental setup consisting of blue LED irradiation from below, first passed through a mask, probing the blend with a red Raman laser using a confocal Raman objective lens. (b) 3D confocal Raman map revealing the binary phase morphology of an acrylate/silicone blend, with an acrylate-rich center. (c) Loss of silicone from the irradiated region owing to phase separation, as revealed by the decrease in the Raman intensity associated with the silicone over time along the depth of the blend. Adapted with permission from ref 62. Copyright 2017 American Chemical Society.

At this point studies on correlating the binary phase morphology of a polymer blend to spontaneous unmasked filamentation remains an open question; indeed, at this point binary filament phases have only been observed with the use of a one-dimensional mask. Future studies might also examine the inclusion of nanoparticles that provide the noise to stimulate the filamentation, as shown in single-component systems.<sup>61</sup> On the basis of the inherent challenges with not using a mask, subsequent studies focused on examining the correlation of binary phase morphology to the self-trapping of arrays of individual beams in order to more easily understand the underlying processes at the single-beam level. The arrays of beams are generated by passing light through a mask consisting of apertures (holes) of a particular diameter, D, and arranged on a square array of spacing, S, and whose configuration is expressed by the ratio D/S. Figure 10 shows the resultant morphologies of a binary polymer blend made from a triacrylate and a short-chain silicone oligomer using a 40/200 mask.<sup>62</sup> These structures were formed as a function of the relative weight fractions of each component, as well as radiation intensity. Specific relative weight fractions as well as irradiation intensities lead to a filament-based structure that spatially correlates to the array of optical beams. The filaments are approximately 40  $\mu$ m in diameter and are arranged in a square array of 200  $\mu$ m spacing, matching the mask pattern used. For the same relative weight fraction, higher intensities can still induce a correlated structure; however the inhibition of phase separation as indicated by the low contrast in the bright and dark regions indicates that the cross-linking might be too high to allow for any phase separation to occur. No shrinkage was observed for these samples. For high relative weight fractios, filaments which are colored blue (owing to the blue LED light used to induce filamentation) are observed; however, they are no longer as correlated to the optical mask. This would also indicate that with a higher fraction of the acrylate the growth of the acrylate phase might allow the filament phases to evolve so more such that they no longer correlate patterned arrays of beams that stimulate their formation. This is confirmed for 50/50 blends in which the binary phase morphology appears random. These results reveal the inherent competition in the process which is varied by the determinative factors, namely the irradiation intensity and the

relative weight fractions of the polymers, which varies the competitive forces of phase separation and photo-cross-linking and dictates whether or not the morphology is spatially congruent to the optical pattern.

While the final structures reveal much about the formation processes and how to control them, it is important to gain an understanding of the underlying formation kinetics and thermodynamics associated with phase separation. To this end, spatially and temporally resolved in situ studies were conducted using confocal Raman spectroscopy to track the conversion as well as phase separation during irradiation. Figure 11a shows the experimental setup that combines both a blue LED that irradiates the polymer blend from below and a confocal Raman objective (red laser) that probes the blend along the propagation direction of a single optical beam. A confirmation of binary phase morphology with one component comprising the filaments and the other the surrounding regions is revealed by 3D Raman volume maps of the Raman peak ratios of the two components (Figure 11b). The temporal evolution of the phase separation of the silicone from the filament is also indicated by the decrease in the silicone Raman peak intensity, which correlates with concentration, over the depth of the blend in the region of the filament over time (Figure 11c).

These *in situ* studies specifically revealed the underlying processes and how directed phase separation creates a binary phase morphology similar to the pattern of the optical beams. Namely, self-trapping first begins in the blend, followed by phase separation, which first begins at the front of the blend and then over the course of polymerization with increased molecular weight, subsequent depths become unstable, and phases separate. Hence there is a frontal aspect to the initiation of these phenomena, as well as a coaxial nature to the dynamics of phase separation and the inherent influx of monomer into the filament to proceed with the growth, although an analysis of the diffusion of monomer into the filament has yet to be examined. Simulations of light self-trapping blends over a range of reactivity and  $\chi$  values also confirm the competition between phase separation and cross-linking in determining morphology.  $^{60}$ 

The binary phase morphologies are essentially arrays of microscale vertically aligned fiber optics, as they comprise a core-cladding architecture of cylindrical geometry and two

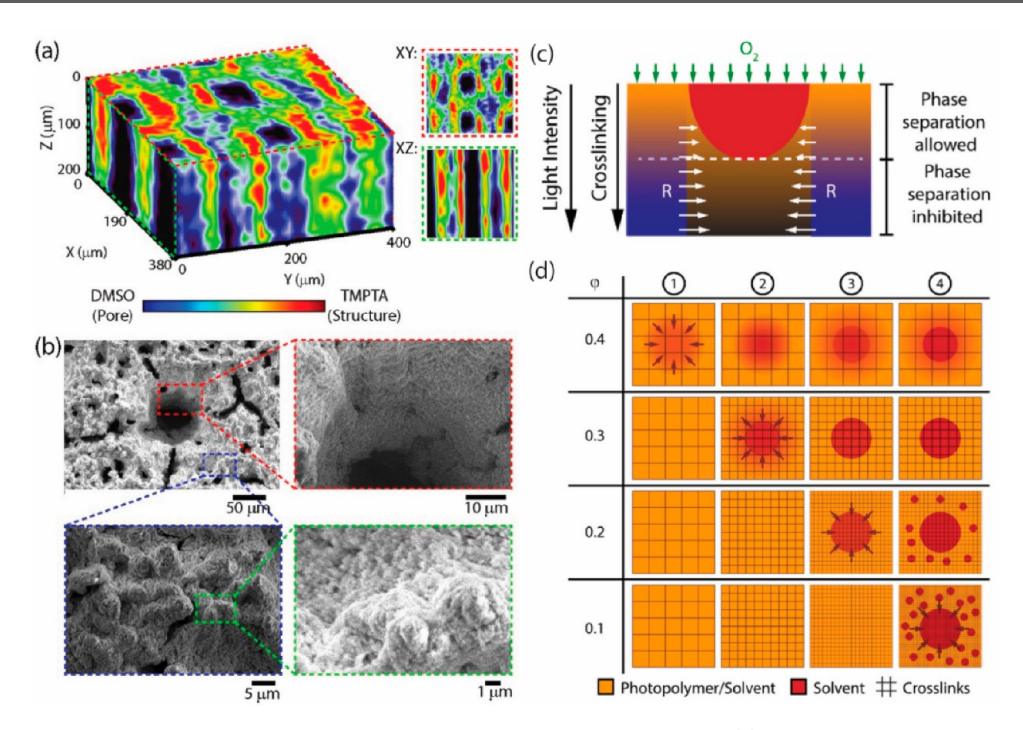
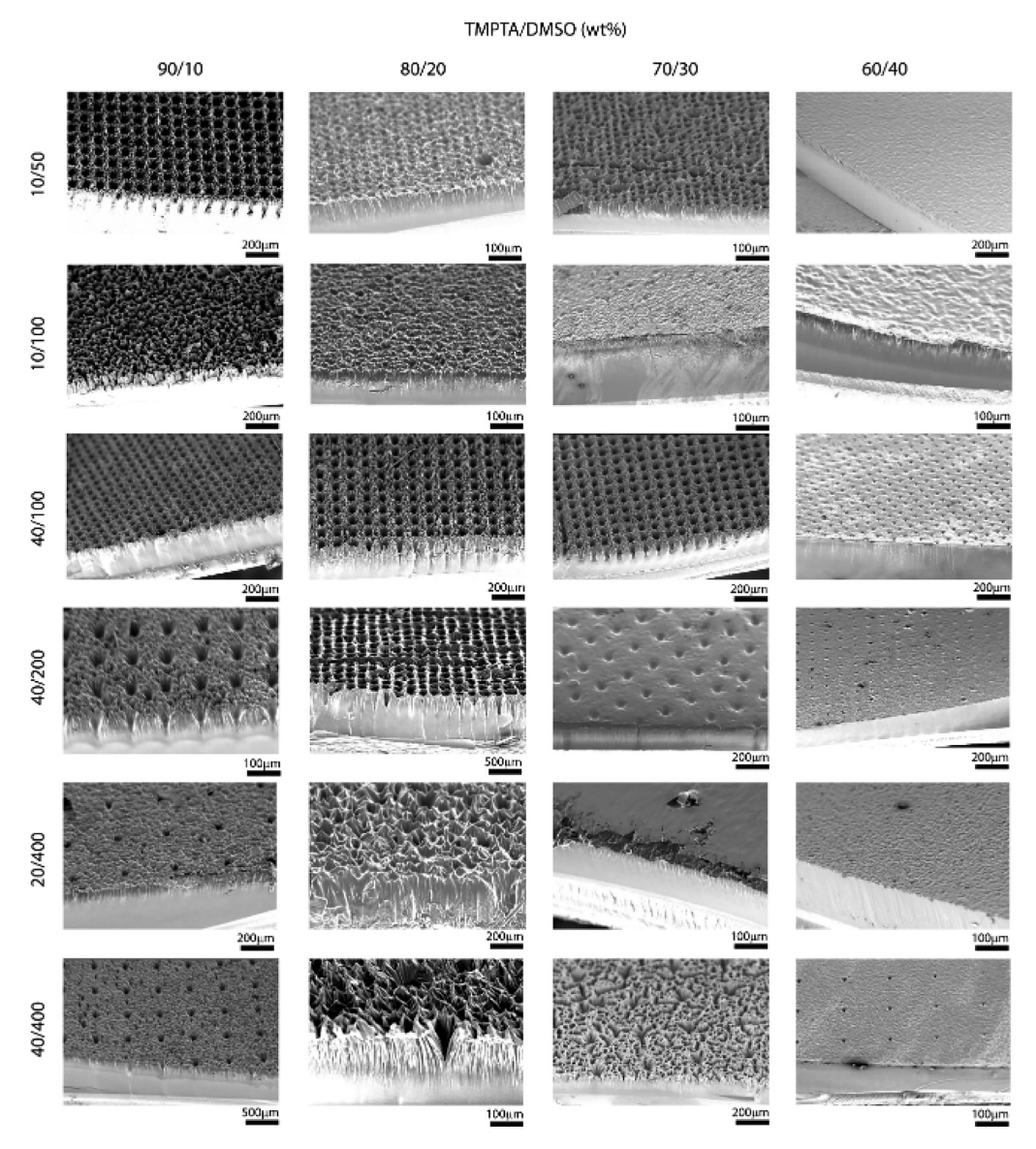


Figure 12. Formation of a microporous surface structure in a photopolymer—solvent mixture. (a) Raman 3D map showing the phase-separated arrangement of polymer and solvent. (b) SEM images of the pore formation, as well as the texture afforded by a nanoparticle coating. (c) Schematic of the process of phase separation including diffusion of oxygen from the ambient atmosphere, a gradient in light intensity due to photoabsorption, and a gradient in the cross-linking degree (orange to blue). (d) Schematic of the evolution of the phase separation over time as a function of the weight fraction of the photopolymer and how it leads to different phase-separated arrangements on the basis of the cross-linking density. Adapted with permission from ref 29. Copyright 2018 American Chemical Society.

materials with difference refractive indices. Hence, they also found applications as light-capturing and light-collection coatings. Particularly, they have been examined as coatings for solar cells, in which the wider collection window of the arrays of waveguides enables the collection of greater quantities of light in silicon solar cells, which increases both the external quantum efficiency and the output current.<sup>30</sup> These two performance criteria could be optimized through varying the filament size and spacing as well as the relative weight fractions of the components, the last of which improves the contiguous nature of the filaments, which is favorable for waveguiding.<sup>26</sup> Further enhancements were also found when silver nanoparticles were grown in situ via photochemical reduction of a silver salt, producing metallo-dielectric waveguides with wider collection windows owing to the enhancement from nanoparticle scattering.<sup>28</sup>

3.4. Photopolymer-Solvents. Studies have also focused on examining light-directed organization and light self-trapping in photopolymer-solvent mixtures. The approach is similar to that of polymer blends, now coupling light self-trapping to polymerization-induced phase separation of the photopolymersolvent mixtures. Recent studies showed that triacrylate-DMSO mixtures exposed to an inverted optical pattern, namely one with dark spots in an otherwise bright intensity pattern, resulted in filamentation of light in the bright regions. The photopolymer-solvent mixture was found to undergo phase separation, with an organization of the components similar to the light pattern, namely the acrylate comprising the bright regions, and the DMSO solvent phase separating into the dark regions (Figure 12a). Photopolymer-solvent mixtures are commonly employed such that the solvent acts a porogen which is subsequently removed to create porous microstructures. The self-trapping of light produced porous structures with the pore size and space correlating with the light pattern (Figure 12b). The porous structure was only formed at the top surface (away from the light source), with the bottom of the material being completely cross-linked and showing no structure. This would indicate a depth dependence of the process of phase separation (Figure 12c). It was apparent that oxygen exposure to the top surface of the mixture allowed a reduction in the photo-cross-linking, which enabled phase separation to occur, whereas at the bottom of the mixture a lack of inhibition allowed cross-linking to completely stop phase separation. Even within the range of parameters explored, the different pore arrangements could be explained by the crosslinking degree as a function of the weight fraction of photopolymer (Figure 12d). It was concluded that, within the parameters explored, the process could only organize surface structures. An interesting finding was that the pores also formed within the photopolymer matrix: namely, a solvent phase separated not just in the primary pores defined by the mask but if the phase separation was strong DMSO would separate from the photopolymer before reaching the pores. Hence, pore distributions consisting of both the primary pores and these smaller pores could be achieved through tuning the relative weight fractions of the polymer and solvent, as well as the mask. The mask specifically changes the size and spacing of the primary pores, which changes the travel lengths for DMSO to reach them, which could result in he DMSO phase separating before reaching the pores.

Figure 13 shows a mapping of the structure of the microporous substrates over a range of mask patterns as well as relative weight fractions of polymer/DMSO. A range of micropore surface structures could be produced by changing the



**Figure 13.** Microporous surface structures created from the irradiation of photopolymer/solvent mixtures. Structures are mapped over a range of mask patterns and relative weight fractions. Mask patterns are defined as the ratio of the mask's pattern (circular hole) diameter (D) and array spacing (S) and are expressed as D/S. Reprinted with permission from ref 29. Copyright 2018 American Chemical Society.

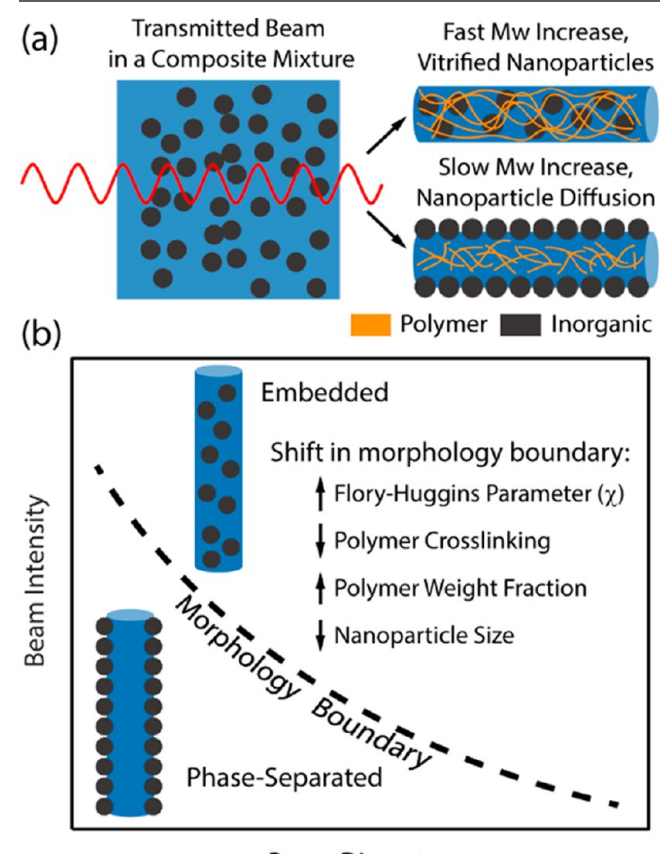
mask. Once again, the principles of competing photo-crosslinking and phase separation led to the organization of the pores. The range of structures that can be produced is very clear, spanning from very smooth surfaces with the primary pores produced from the mask to hierarchical structures in which there is a presence of both the primary pores and nanoscale pores in the matrix to finally random microporous structures bearing no resemblance to the mask pattern. Future studies should examine how the phase separation could be elicited over the entire depth of the mixture, with the potential to produce membranes whose pores permeate the entire thickness of the materials. Additionally, in the future, further work should examine the extent to which light can be used to direct the morphology of polymersolvent mixtures: for example, looking at the extent to which the pore size can be made smaller or larger, the area number density of pores and their arrangement, etc. The range of polymers should also be expanded in order to generalize the process.

3.5. Self-Writing in Complex Media, with Nanoparticles as an Example. The present achievements with

using light self-trapping to produce structures in single polymer components, polymer blends, and polymer solvent mixtures naturally leads to interest in generalizing the process to the organization of additional complex formulations. Indeed, this is the long-term goal of the author: to leverage light-stimulated dynamics to organize a broad range of multicomponent materials. Future work should examine the organization of materials with higher complexity in terms of more components, as well as to compositions moving toward the hybrid organicinorganic or even purely inorganic systems. One example is to examine organization of polymer-nanoparticle composite materials, which are important precursor formulations toward the production of a range of important materials and coatings used in many applications. In the short term, for example, we are beginning to examine light self-writing in photopolymernanoparticle formulations. The general expectation is for such systems to emulate processes similar to those observed in polymer blends: namely, that there is processing parameter space in which phase-separated structures can be produced, as

well as one that produces homogeneous structures in which the nanoparticles are embedded in the filament (i.e., lack of phase separation). Previous studies have shown that photopolymer nanoparticle formulations can undergo self-trapping, <sup>61,63</sup> with the presence of the nanoparticles not being deleterious to the process. Our recent work on the in situ production of nanoparticles in filaments is also a step in this general direction. <sup>28</sup>

Figure 14a illustrates these two expected general types of morphologies (examined after full curing of the formulation)



Beam Diameter

**Figure 14.** Proposal for self-writing composites from photopolymer–nanoparticle formulations. (a) Principle for the formation of embedded and core—shell morphologies based on the rate of growth in the polymer molecular weight. (b) Hypothesized parameter space consisting of a morphology boundary separation the two morphologies. Arrows indicate the expected shift in the boundary with increase in one of four different parameters of the photocurable mixtures.

and how the different mixture and processing parameters would result in producing either of the two. It is expected that the competition between phase separation and photo-cross-linking, observed in prior work, will result in core—shell or "embedded" structures. A fast increase in molecular weight will vitrify the nanoparticles in the polymer matrix. Slower growth will allow them to be expelled from the forming filament. In such studies there are numerous parameters that could be examined in terms of their dependence or effect on the final morphology, specifically parameters that affect both phase separation and/or photo cross-linking. Figure 14b proposes a morphology map in which the two primary axes are beam intensity and beam diameter. A morphology boundary separates this two-variable parameter space into regions in which it can be expected to

produce core-shell or embedded structures. For example, at very low intensities and small beam diameters the growth in the molecular weight and cross-linking of the filament will not be sufficient to inhibit phase separation, and the smaller diameter specifically reduces the path length nanoparticles must diffuse to exit the filament region, easily resulting in core—shell structures. On the other hand, very high intensity beams that are also larger will increase both the diffusion path length over which a nanoparticle must travel to reach the periphery and the rate at which the molecular weight and cross-linking increases, thereby quickly inhibiting diffusion and reducing the quantity of nanoparticles that can leave the filament, leading to embedded structures. This parameter space envisions that the boundary between the two morphologies will shift up and down or left and right but still retain its general shape in separating embedded and phase-separated morphologies from the upper right to the lower left, respectively. The effects of other parameters, such as  $\chi$ and weight fraction and even particle size, are proposed in Figure 14b as to how they will shift the boundary. Nanoparticles may also be synthesized in situ during the self-writing process, enabling possibly high- $\chi$  systems to be organized.<sup>28</sup>

## 4. OUTLOOK AND OUTSTANDING QUESTIONS AND AREAS OF INOUIRY

Significant progress has been made over the past two decades in exploiting and leveraging the principles of self-trapping in photoreactive systems toward examining complex nonlinear optical phenomena, and nonlinear dynamics in soft systems. However, there are a diverse range of research areas that are critical to fundamentally understand both the process and the underlying reaction, diffusion, and dynamics, toward generalizing the method as well as seeking opportunities to organize more complex compositions. This section summarizes some open opportunities for further investigation.

The macromolecular origins of the intensity dependence as well as the interaction of light with growing polymer should be closely examined, with both experimental and theoretical approaches. Correlations of polymer molecular structure, refractive index, and self-trapping can avail themselves of the progress with engineering high-index polymers to draw principles on correlating molecular weight and structure to refractive index. 64,65 In light of the importance of this coupling of light to polymer growth, studies should examine a closer correlation of exactly how the increase in refractive index correlates to polymer growth, as well as dependences on the actual chemical structure of the monomer, molecular weight, and other types of macromolecular structures, such as crosslinking or branching. Specifically, studies should elucidate the specific value of the refractive index as a function of the current state of the molecular structure of the polymer. Kinetic studies should also focus on correlating conversion of the polymer with the refractive index, to elucidate the actual trend in the rise of nversus polymer structure (e.g., molecular weight).

Exploration of other material systems should also be pursued, to demonstrate organization of a broad range of systems. Indeed, self-trapping has been observed, for example, in photosensitive glasses, <sup>66,67</sup> indicating the potential applicability to inorganic systems, in addition to polymer—inorganic systems. Even within polymer systems themselves, a wider range of compositions should be examined, especially functional polymers, e.g. conducting and thermoelectric, to investigate attractive structure—property correlations. Employing a broader range of polymers can also aid in further confirming hypotheses on the

correlation of the underlying processes and resultant morphology for such aspects as polymer reactivity, polymer composition, relative weight fraction, and miscibility. Another avenue is to examine ternary polymer blends, to examine multiple stages of phase separation among the three components.

It is also desirable to produce structures with smaller scale features, specifically toward microscale structures in which the filaments are less than one micrometer. Theoretical predictions placed the smallest self-trapped beam to be less than 1  $\mu$ m. However, this requires coherent sources, which may obviate the inherent benefits of scalability and low cost by currently using incandescent sources or LEDs. However, the benefits of producing micro scale structures might make it worth constructing an experimental setup with coherent light sources.

Another path toward scalability is to demonstrate that these structures can be produced in some type of continuous fashion. Toward this end, attempts could be made to produce the structures on a conveyor belt type system in which the structures are continuously produced. Indeed, previous computational work has demonstrated the potential to control polymer blend morphology on continuous lines, <sup>68,69</sup> which is promising when this is integrated with MI using a single source to achieve randomly positioned filaments or multiple sources to create 2D or 3D periodic structures. Hence, modulation instability is the key to scalability. Studies to achieve the directed organization of composites using MI should also be pursued. This might entail more careful compositional programming of the formulation to ensure that the filaments form by themselves, as well as the capability for filament evolution to then facilitate phase separation.

New forms of nonlinearity should also be examined in polymer systems. The essential aspect is that any change to the polymer structure will change its refractive index. Hence it is possible to examine photomechanical changes to the polymer structure and how it relates to changes in the refractive index, as a new form of nonlinearity. Light-induced depolymerization and de-cross-linking are also possibilities, which would lead to a decrease in refractive index, but a change, nonetheless. The use of liquid crystals and plasmatic nanoparticles might also aid in providing nonlinearity in such photosensitive polymer systems. 61

#### 5. CONCLUSION

This perspective presented the idea of leveraging nonlinear optical phenomena, observed originally in inorganic systems and now in soft systems, particularly photoreactive polymers, toward examining the possibilities of nonlinear optical pattern formation as well as materials organization. Achievements over the past two decades have shown that this is possible to produce and organize materials, soft materials, using this process. As well, significant achievements in demonstrating favorable material properties and material structures substantiates this process as one that should be advanced to produce a wider range of functional material structures, and further studies on the underlying processes underpinning the technique should be pursued. Light-induced self-writing and nonlinear optical pattern formation in photosensitive polymer systems bridges two very distinct fields. It is often at the intersection of such distinct fields where interesting phenomena emerge. Continued work in this broad area would allow these phenomena to converge toward a generalizable approach toward materials organization, as well as reveal new concepts in materials organization.

#### AUTHOR INFORMATION

#### **Corresponding Author**

Ian D. Hosein — Syracuse University, Department of Biomedical and Chemical Engineering, Syracuse, New York 13244, United States; ocid.org/0000-0003-0317-2644; Email: idhosein@syr.edu

Complete contact information is available at: https://pubs.acs.org/10.1021/acs.chemmater.9b05373

#### **Notes**

The author declares no competing financial interest.

#### **Biography**

Dr. Ian D. Hosein received his Bachelor in Applied Science in 2000 from the University of Toronto, Toronto, Canada. He obtained his Ph.D. in Materials Science & Engineering from Cornell University in 2009. He is an assistant professor in the Department of Biomedical & Chemical Engineering at Syracuse University. His research interests are in creating new materials processing routes towards new structures and the discovery of novel structure—property correlations and their application toward preparing functional materials.

### ACKNOWLEDGMENTS

The works of I.D.H. described herein were supported by the Syracuse Center of Excellence (SU-COE), the National Science Foundation under Grant Agreement number CMMI-1751621, the American Chemical Society under Grant Agreement number PRF# 57332-DNI7, the 3M Foundation (NTFA award), and the College of Engineering and Computer Science at Syracuse University.

#### **■** REFERENCES

- (1) Odian, G. G. Principles of Polymerization, 3rd ed.; Wiley: New York, 1991.
- (2) Pojman, J. A. Nonlinear Chemical Dynamics in Synthetic Polymer Systems. *Nato Sci. Peace Sec A* **2009**, 221–240.
- (3) Pojman, J. A.; Tran-Cong-Miyata, Q. Nonlinear Dynamics in Polymeric Systems; American Chemical Society: 2003; Vol. 869, p 380.
- (4) Masere, J.; Pojman, J. A. Free radical-scavenging dyes as indicators of frontal polymerization dynamics. *J. Chem. Soc., Faraday Trans.* **1998**, 94, 919–922.
- (S) Shukutani, T.; Myojo, T.; Nakanishi, H.; Norisuye, T.; Qui, T. C. M. Tricontinuous Morphology of Ternary Polymer Blends Driven by Photopolymerization: Reaction and Phase Separation Kinetics. *Macromolecules* **2014**, *47*, 4380–4386.
- (6) Maeda, S.; Hara, Y.; Yoshida, R.; Hashimoto, S. Peristaltic Motion of Polymer Gels. *Angew. Chem., Int. Ed.* **2008**, *47*, 6690–6693.
- (7) Xue, L.; Han, Y. Pattern formation by dewetting of polymer thin film. *Prog. Polym. Sci.* **2011**, *36*, 269–293.
- (8) Kewitsch, A. S.; Yariv, A. Self-focusing and self-trapping of optical beams upon photopolymerization. *Opt. Lett.* **1996**, *21*, 24–26.
- (9) Frisken, S. J. Light-induced optical waveguide uptapers. *Opt. Lett.* **1993**, *18*, 1035–1037.
- (10) Trillo, S.; Torruellas, W. Spatial Solitons; Springer: Berlin, 2001.
- (11) Chiao, R. Y.; Garmire, E.; Townes, C. H. Self-Trapping of Optical Beams. *Phys. Rev. Lett.* **1964**, *13*, 479–482.
- (12) Monro, T. M.; De Sterke, C. M.; Poladian, L. Catching light in its own trap. *J. Mod. Opt.* **2001**, *48*, 191–238.
- (13) Biria, S.; Morim, D. R.; An Tsao, F.; Saravanamuttu, K.; Hosein, I. D. Coupling nonlinear optical waves to photoreactive and phase-separating soft matter: Current status and perspectives. *Chaos* **2017**, 27, 104611.
- (14) Askadskii, A. A. Influence of crosslinking density on the properties of polymer networks. *Polym. Sci. U.S.S.R.* **1990**, 32, 2061–2069.

- (15) Decker, C. The use of UV irradiation in polymerization. *Polym. Int.* **1998**, *45*, 133–141.
- (16) Decker, C.; Moussa, K. Real-Time Kinetic-Study of Laser-Induced Polymerization. *Macromolecules* **1989**, 22, 4455–4462.
- (17) Biria, S.; Malley, P. P. A.; Kahan, T. F.; Hosein, I. D. Optical Autocatalysis Establishes Novel Spatial Dynamics in Phase Separation of Polymer Blends during Photocuring. *ACS Macro Lett.* **2016**, *5*, 1237–1241.
- (18) Pojman, J. A.; Ilyashenko, V. M.; Khan, A. M. Free-radical frontal polymerization: Self-propagating thermal reaction waves. *J. Chem. Soc., Faraday Trans.* **1996**, *92*, 2825–2837.
- (19) Fouassier, J.-P.; Rabek, J. F. Radiation Curing in Polymer Science and Technology; Elsevier: London, 1993; Vols. 1-4.
- (20) Fouassier, J. P.; Lalevée, J. Photoinitiators for Polymer Synthesis: Scope, Reactivity, and Efficiency; Wiley: Donauwörth, 2013.
- (21) Kagami, M.; Yamashita, T.; Ito, H. Light-induced self-written three-dimensional optical waveguide. *Appl. Phys. Lett.* **2001**, *79*, 1079–1081.
- (22) Zhang, J. H.; Kasala, K.; Rewari, A.; Saravanamuttu, K. Self-trapping of spatially and temporally incoherent white light in a photochemical medium. *J. Am. Chem. Soc.* **2006**, *128*, 406–407.
- (23) Chen, F. H.; Pathreeker, S.; Biria, S.; Hosein, I. D. Synthesis of Micropillar Arrays via Photopolymerization: An in Situ Study of Light-Induced Formation, Growth Kinetics, and the Influence of Oxygen Inhibition. *Macromolecules* **2017**, *50*, 5767–5778.
- (24) Li, H.; Chen, F.-H.; Biria, S.; Hosein, I. D. Prototyping of Superhydrophobic Surfaces from Structure-Tunable Micropillar Arrays Using Visible Light Photocuring. *Adv. Eng. Mater.* **2019**, *21*, 1801150.
- (25) Shoji, S.; Kawata, S. Optically-induced growth of fiber patterns into a photopolymerizable resin. *Appl. Phys. Lett.* **1999**, *75*, 737–739.
- (26) Biria, S.; Chen, F.-H.; Hosein, I. D. Enhanced Wide-Angle Energy Conversion Using Structure-Tunable Waveguide Arrays as Encapsulation Materials for Silicon Solar Cells. *Phys. Status Solidi A* **2019**, *216*, 1800716.
- (27) Lin, H.; Biria, S.; Chen, F.-H.; Hosein, I. D.; Saravanamuttu, K. Waveguide-imprinted slim polymer films: beam steering coatings for solar cells. *ACS Photonics* **2019**, *6*, 878–885.
- (28) Biria, S.; Wilhelm, T. S.; Mohseni, P. K.; Hosein, I. D. Direct Light-Writing of Nanoparticle-Based Metallo-Dielectric Optical Waveguide Arrays Over Silicon Solar Cells for Wide-Angle Light Collecting Modules. *Adv. Opt. Mater.* **2019**, *7*, 1900661.
- (29) Biria, S.; Hosein, I. D. Superhydrophobic Microporous Substrates via Photocuring: Coupling Optical Pattern Formation to Phase Separation for Process-Tunable Pore Architectures. *ACS Appl. Mater. Interfaces* **2018**, *10*, 3094–3105.
- (30) Biria, S.; Chen, F. H.; Pathreeker, S.; Hosein, I. D. Polymer Encapsulants Incorporating Light-Guiding Architectures to Increase Optical Energy Conversion in Solar Cells. *Adv. Mater.* **2018**, *30*, 1705382.
- (31) Biria, S.; Malley, P. P. A.; Kahan, T. F.; Hosein, I. D. Tunable Nonlinear Optical Pattern Formation and Microstructure in Cross-Linking Acrylate Systems during Free-Radical Polymerization. *J. Phys. Chem. C* **2016**, *120*, 4517–4528.
- (32) Basker, D. K.; Brook, M. A.; Saravanamuttu, K. Spontaneous Emergence of Nonlinear Light Waves and Self-Inscribed Waveguide Microstructure during the Cationic Polymerization of Epoxides. *J. Phys. Chem. C* **2015**, *119*, 20606–20617.
- (33) Burgess, I. B.; Shimmell, W. E.; Saravanamuttu, K. Spontaneous pattern formation due to modulation instability of incoherent white light in a photopolymerizable medium. *J. Am. Chem. Soc.* **2007**, *129*, 4738–4746.
- (34) Zhang, J. H.; Saravanamuttu, K. The dynamics of self-trapped beams of incoherent white light in a free-radical photopolymerizable medium. *J. Am. Chem. Soc.* **2006**, *128*, 14913–14923.
- (35) Saravanamuttu, K.; Zhang, J. H.; Sakalauskas, M.; Kasala, K. Self-trapped white light beams and their interactions in a Photochemical system. *Abstr. Pap. Am. Chem. Soc.* **2006**, 232, 473–473.
- (36) Villafranca, A. B.; Saravanamuttu, K. An Experimental Study of the Dynamics and Temporal Evolution of Self-Trapped Laser Beams in

- a Photopolymerizable Organosiloxane. J. Phys. Chem. C 2008, 112, 17388-17396.
- (37) Zhao, G. H.; Mouroulis, P. Diffusion-Model of Hologram Formation in Dry Photopolymer Materials. *J. Mod. Opt.* **1994**, *41*, 1929–1939.
- (38) Sheridan, J. T.; Downey, M.; O'Neill, F. T. Diffusion-based model of holographic grating formation in photopolymers: generalized non-local material responses. *J. Opt. A: Pure Appl. Opt.* **2001**, *3*, 477–488.
- (39) Ben Belgacem, M.; Kamoun, S.; Gargouri, M.; Honorat Dorkenoo, K. D.; Barsella, A.; Mager, L. Light induced self-written waveguides interactions in photopolymer media. *Opt. Express* **2015**, 23, 20841–20848.
- (40) Li, H.; Qi, Y.; Malallah, R. e.; Sheridan, J. T. Modeling the nonlinear photoabsorptive behavior during self-written waveguide formation in a photopolymer. *J. Opt. Soc. Am. B* **2015**, *32*, 912–922.
- (41) Ponte, M. R.; Welch, R.; Saravanamuttu, K. An optochemically organized nonlinear waveguide lattice with primitive cubic symmetry. *Opt. Express* **2013**, *21*, 4205–4214.
- (42) Kasala, K.; Saravanamuttu, K. Optochemical self-organisation of white light in a photopolymerisable gel: a single-step route to intersecting and interleaving 3-D optical and waveguide lattices. *J. Mater. Chem.* **2012**, 22, 12281–12287.
- (43) Burgess, I. B.; Ponte, M. R.; Saravanamuttu, K. Spontaneous formation of 3-D optical and structural lattices from two orthogonal and mutually incoherent beams of white light propagating in a photopolymerisable material. *J. Mater. Chem.* **2008**, *18*, 4133–4139.
- (44) Kasala, K.; Saravanamuttu, K. Optochemical Organization in a Spatially Modulated Incandescent Field: A Single-Step Route to Black and Bright Polymer Lattices. *Langmuir* **2013**, *29*, 1221–1227.
- (45) Ponte, M. R.; Hudson, A. D.; Saravanamuttu, K. Self-Organized Lattices of Nonlinear Optochemical Waves in Photopolymerizable Fluids: The Spontaneous Emergence of 3-D Order in a Weakly Correlated System. *J. Phys. Chem. Lett.* **2018**, *9*, 1146–1155.
- (46) Hosein, I. D.; Lin, H.; Ponte, M. R.; Basker, D.; Saravanamuttu, K. Multidirectional waveguide arrays in a planar architecture. *Organic Photonic Materials and Devices XVI*; 2014, 8983.
- (47) Hosein, I. D.; Lin, H.; Ponte, M. R.; Basker, D. K.; Saravanamuttu, K. In Enhancing Solar Energy Light Capture with Multi-Directional Waveguide Lattices. *Renewable Energy and the Environment*, Tucson, AZ, 2013/11/03; Optical Society of America: Tucson, AZ, 2013; p RM2D.2.
- (48) Hosein, I. D.; Lin, H.; Ponte, M. R.; Basker, D. K.; Brook, M. A.; Saravanamuttu, K. Waveguide Encoded Lattices (WELs): Slim Polymer Films with Panoramic Fields of View (FOV) and Multiple Imaging Functionality. *Adv. Funct. Mater.* **2017**, *27*, 1702242.
- (49) Lin, H.; Hosein, I. D.; Benincasa, K. A.; Saravanamuttu, K. A Slim Polymer Film with a Seamless Panoramic Field of View: The Radially Distributed Waveguide Encoded Lattice (RDWEL). *Adv. Opt. Mater.* **2019**, *7*, 1801091.
- (50) Lin, H.; Benincasa, K. A.; Fradin, C.; Saravanamuttu, K. Shaping LED Beams with Radially Distributed Waveguide-Encoded Lattices. *Adv. Opt. Mater.* **2019**, *7*, 1801487.
- (51) Chen, F. H.; Pathreeker, S.; Kaur, J.; Hosein, I. D. Increasing light capture in silicon solar cells with encapsulants incorporating air prisms to reduce metallic contact losses. *Opt. Express* **2016**, *24*, A1419—A1430.
- (52) Chen, F.-H.; Biria, S.; Li, H.; Hosein, I. D. Microfiber Optic Arrays as Top Coatings for Front-Contact Solar Cells toward Mitigation of Shading Loss. ACS Appl. Mater. Interfaces 2019, 11, 47422–47427.
- (53) Hudson, A. D.; Ponte, M. R.; Mahmood, F.; Pena Ventura, T.; Saravanamuttu, K. A soft photopolymer cuboid that computes with binary strings of white light. *Nat. Commun.* **2019**, *10*, 2310.
- (54) Morim, D. R.; Meeks, A.; Shastri, A.; Tran, A.; Shneidman, A. V.; Yashin, V. V.; Mahmood, F.; Balazs, A. C.; Aizenberg, J.; Saravanamuttu, K. Opto-chemo-mechanical transduction in photoresponsive gels elicits switchable self-trapped beams with remote interactions. *Proc. Natl. Acad. Sci. U. S. A.* **2020**, *117*, 3953.

- (55) Tran-Cong-Miyata, Q.; Nakanishi, H. Phase separation of polymer mixtures driven by photochemical reactions: current status and perspectives. *Polym. Int.* **2017**, *66*, 213–222.
- (56) Smith, D. M.; Li, C. Y.; Bunning, T. J. Light-Directed Mesoscale Phase Separation via Holographic Polymerization. *J. Polym. Sci., Part B: Polym. Phys.* **2014**, *52*, 232–250.
- (57) Bauer, B. J.; Briber, R. M., The effect of crosslink density on phase separation in interpenetrating polymer networks. In *Advances in interpenetrating polymer networks*; Klempner, D., Frisch, K., Eds.: CRC Press: Lancaster, PA, 1994; Vol. 4, p 45.
- (58) Flory, P. J.; Rehner, J. Statistical mechanics of cross-linked polymer networks II Swelling. *J. Chem. Phys.* **1943**, *11*, 521–526.
- (59) Flory, P. J. Principles of Polymer Chemistry; Cornell University Press: Ithaca, NY, 1953.
- (60) Biria, S.; Hosein, I. D. Simulations of Morphology Evolution in Polymer Blends during Light Self-Trapping. *J. Phys. Chem. C* **2017**, *121*, 11717—11726
- (61) Qiu, L. Q.; Saravanamuttu, K. Optical self-trapping in a photopolymer doped with Ag nanoparticles: a single-step route to metallodielectric cylindrical waveguides. *J. Opt. Soc. Am. B* **2012**, 29, 1085–1093.
- (62) Biria, S.; Hosein, I. D. Control of Morphology in Polymer Blends through Light Self-Trapping: An in Situ Study of Structure Evolution, Reaction Kinetics, and Phase Separation. *Macromolecules* **2017**, *50*, 3617–3626.
- (63) Qiu, L. Q.; Saravanamuttu, K. Modulation instability of incandescent light in a photopolymer doped with Ag nanoparticles. *J. Opt.* **2012**, *14*, 125202.
- (64) Higashihara, T.; Ueda, M. Recent Progress in High Refractive Index Polymers. *Macromolecules* **2015**, 48, 1915–1929.
- (65) Badur, T.; Dams, C.; Hampp, N. High Refractive Index Polymers by Design. *Macromolecules* **2018**, *51*, 4220–4228.
- (66) Ljungstrom, A.M.; Monro, T.M. Light-Induced Self-Writing Effects in Bulk Chalcogenide Glass. J. Lightwave Technol. 2002, 20, 78.
- (67) Monro, T. M.; Moss, D.; Bazylenko, M.; de Sterke, C. M.; Poladian, L. Observation of self-trapping of light in a self-written channel in a photosensitive glass. *Phys. Rev. Lett.* **1998**, *80*, 4072–4075.
- (68) Travasso, R. D. M.; Kuksenok, O.; Balazs, A. C. Exploiting Photoinduced Reactions in Polymer Blends to Create Hierarchically Ordered, Defect-Free Materials. *Langmuir* **2006**, *22*, 2620–2628.
- (69) Balazs, A. C. Modeling Self-Assembly and Phase Behavior in Complex Mixtures. *Annu. Rev. Phys. Chem.* **2007**, 58, 211–233.